NEW ELECTROMAGNETIC BANDGAP NONLINEAR COPLANAR WAVEGUIDES

Ferran Martín,[1] Francisco Falcone,[2] Jordi Bonache,[1] Txema Lopetegi,[2] Miguel A. G. Laso,[2] J. L. Carreras,[1] and Mario Sorolla[2]
[1] Departament d'Enginyeria Electrònica
Universitat Autónoma de Barcelona
08193 Bellaterra (Barcelona), Spain
[2] Departamento de Ingeniería Eléctrica y Electrónica
Universidad Pública de Navarra
31006 Pamplona, Spain

Received 6 December 2002

ABSTRACT: *In this paper, nonlinear transmission lines (NLTLs) consisting of coplanar waveguides periodically loaded with shunt connected varactor diodes, periodically perturbed by varying the slot width, are studied. To our knowledge, this is the first time that these structures, combining a distributed nonlinearity with an electromagnetic bandgap (EBG), are investigated. A prototype device with a cutoff frequency near 1 GHz and designed to inhibit power transmission within a narrow frequency gap near cutoff has been fabricated. Harmonic balance simulations as well as nonlinear measurements indicate that power transfer to the second harmonic is enhanced if the third harmonic lies within the forbidden gap. The work opens the door to a major design flexibility of NLTL frequency multipliers and phase shifters by adding the EBG concept to the structure.* © 2003 Wiley Periodicals, Inc. Microwave Opt Technol Lett 37: 397–401, 2003; Published online in Wiley InterScience (www.interscience.wiley.com). DOI 10.1002/mop.10929

Key words: *electromagnetic bandgaps (EBGs); nonlinear transmission lines (NLTLs); coplanar waveguide technology; frequency multipliers*

1. INTRODUCTION

Nonlinear transmission lines (NLTLs) are high-impedance transmission media periodically loaded with shunt-connected varactor diodes (Figure 1). Due to nonlinear device grounding, these structures have usually been fabricated in coplanar waveguide (CPW) technology, where the use of vias is not necessary. Moreover, the fact that the wave impedance in CPWs does not univocally determine the lateral dimensions of the structure (strip and slot width) aids design flexibility. Because of their periodicity, NLTLs are also dispersive structures that exhibit passband-stopband characteristics. The first passband is delimited by the Bragg frequency, which is a key parameter for the design of these structures [1]. In recent years, NLTLs have been used for a variety of applications. In the lineal regime, they have been used as time-delay phase shifters in phased-array antennas [2], where a DC bias applied to the shunt-connected Schottky diodes acts as electronic control of phase velocity. NLTLs can be also applied to the design of compact lowpass filters since due to the presence of varactors (and hence dispersion) a slow wave transmission media results. Under large-signal conditions, impulse compression [3], pico-second pulse generation, and harmonic generation [4, 5] have been achieved through the combined effects of nonlinearity and dispersion, which give rise to soliton-like propagation [6].

Several works have focused on the optimisation of NLTLs as frequency multipliers [1, 7, 8]. In this regard, the nonlinear device plays a fundamental role, because it has a direct influence on a key parameter for harmonic generation, namely, conversion efficiency [9]. However, a further flexibility of design can be potentially achieved by introducing the electromagnetic bandgap (EBG) concept [10] to the NLTL. EBGs, also called electromagnetic crystals, are periodic structures which exhibit a frequency-selective behaviour similar to carrier transport in semiconductors. These are

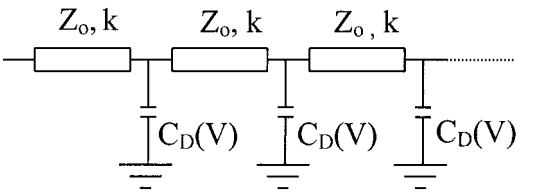

Figure 1 Structure of a nonlinear transmission line

transmission-line-based structures with periodic perturbations of wave impedance. Due to this periodicity, rejection in certain frequency regions occurs and thus the selective behaviour of the structure arises. According to coupled-mode theory, the rejected bands are roughly given by the spectrum of the coupling coefficient [11, 12], which is closely related to the spatial variation of wave impedance and, hence, line geometry. EBG structures have been successfully applied to the elimination of spurious bands in distributed band-pass filters [13]. Also, EBGs have been applied to broadband power amplifiers [14] and oscillators [15] in order to enhance efficiency and reduce phase noise, respectively. In the cited applications, the devices have been fabricated in microstrip technology, where wave impedance is modulated by drilling holes in the substrate, by etching holes in the ground plane, or by varying the lateral dimensions of the transmission lines. The net effect is a perturbation of the effective dielectric constant and impedance of the line.

Regarding the application of EBGs to coplanar waveguide technology, few structures have been reported to date. CPW reflectors have been fabricated by etching periodic structures in the ground planes in close proximity to the slots [16]. Also, EBG filters and resonators consisting of CPWs with a square-wave variation of the slot width have been designed and fabricated [17–19]. A miniaturized low-pass filter, based on the slow-wave effect and reflection properties that take place by periodically enhancing the capacitive coupling between the central strip and ground planes, has been proposed [20]. Finally, a spurious free low-pass filter based on periodic loaded CPWs with slot width perturbations has been recently proposed [21, 22]. However, the application of EBGs to nonlinear distributed structures, such as CPW NLTLs, has not been investigated so far. In this work, the EBG concept is applied to nonlinear CPWs periodically loaded with varactor diodes with the aim to control signal propagation in the first frequency band under large signal conditions. To this end, the slot width is periodically varied, thus achieving wave impedance modulation. Under the assumption of an EBG structure with the proper period to generate a frequency gap in the first passband, it is not obvious that the EBG structure will effectively inhibit the propagation of harmonics lying within that gap. This is due to the fact that we are dealing with a distributed nonlinearity, which means that the power transferred to the harmonics is enhanced during propagation, and the phase of those harmonics is not expected to vary linearly along the line. Ideally, for an EBG to be effective, several periods are required in which the phase of the signal to be rejected varies linearly. Because slot-width perturbation in the structures under study is directly applied to the region of distributed nonlinearity, the last condition is not expected to be satisfied. However, as will be shown later, we have found that by creating a frequency gap in the passband of an NLTL by means of an EBG, the power transferred to those harmonics lying within that gap is severely reduced, while the power transferred to lower-order harmonics (not affected by the gap) is enhanced. These results, obtained by computer simulation and experimentally verified, are of interest for the rejection of undesired harmonics in NLTL frequency multipliers, since no additional cascading stages are required.

2. DESIGN OF AN EBG-NLTL STRUCTURE

Before the introduction of the EBG structure to the device, we will first design an unperturbed CPW NLTL periodically loaded with varactor diodes. To this end, it is necessary to set the main electrical parameters, that is, the Bragg frequency f_B, which delimits the operative bandwidth of the device, and the characteristic impedance of the loaded line Z_L (including the presence of varactors). The latter parameter is set to $Z_L = 50\Omega$ in order to minimize insertion loss in the passband, while the Bragg frequency is set to a nominal value of $f_B = 0.75$ GHz. This relatively small value of the cutoff frequency is justified because this work is devoted to explore the possibilities of a combined EBG and NLTL structure, rather than to fabricate a device with specific performance. By choosing this value for f_B, the requirements for the nonlinear devices (such as the self-resonant frequency) are less stringent. The above parameters are related to line parameters by the following equations:

$$Z_L = \sqrt{\frac{L}{C + C_{ls}}} \tag{1}$$

$$f_B = \frac{1}{\pi \sqrt{L(C + C_{ls})}} \tag{2}$$

where C and L are the respective capacitance and inductance of each transmission line section between adjacent diodes, and C_{ls} is the large signal capacitance of these diodes, defined as the average value over peak to peak voltage excursion. It is important to mention that C_{ls} is improperly defined in an NLTL because the harmonic content of the feeding signal varies along the line and hence the signal waveform. However, by biasing the nonlinear devices at the dc voltage corresponding to a capacitance value coincident with C_{ls}, it is expected to fit Z_L and f_B with reasonable approximation. Equation (2) is actually an approximation based on the lumped equivalent model of the NLTL. To be valid, it is necessary that $C_{ls} > C$ [23], a condition that is satisfied in our prototypes, as will be shown later. By inverting the previous equations, we obtain $L = 21.2$ nH, and an overall capacitance of $C + C_{ls} = 8.5$ pF. To determine each capacitance, we have taken into account the dc bias point of the loading devices (BB833-Infineon Technologies silicon tuning diodes disposed in parallel pairs), which has been set to 5 V to allow significant power for the feeding signal while maintaining the devices under reverse conditions. Under this polarity, the capacitance of each individual diode is approximately 3.25 pF; therefore, the large signal capacitance is $C_{ls} = 6.5$ pF and the per-section capacitance is $C = 2$ pF. From these values of L and C, the characteristic impedance of the line without the presence of varactors is found to be $Z_o = 104\Omega$. The prototype devices have been fabricated on a Rogers RO3010 substrate ($\varepsilon_r = 10.2$, thickness $h = 1.27$ mm) without back-side metal to avoid the propagation of parallel plate substrate modes [24]. To determine the layout of the structure, a commercial transmission line calculator has been used. From this, the strip and slot widths of the coplanar waveguide have been found to be $W = 1.6$ mm and $G = 4$ mm, respectively, while consecutive diode pairs are separated a distance $l = 33.9$ mm.

Let us now focus on the design of the EBG NLTL structure. For this, the slot width has been periodically perturbed (leaving the strip width unaltered). It is well known that the period of the perturbation λ_T determines the center frequency of the rejected band f_o, according to the Bragg condition $\lambda_T = \nu_{pL}/2f_o$ (or $\lambda_T = \pi/\beta$), where ν_{pL} is the propagation velocity of the loaded line and β the phase constant. The application of this condition to NLTLs requires some caution since there is significant dispersion near the Bragg frequency, due to the presence of loading reactances. The dispersion relation of the NLTL is given by [25]:

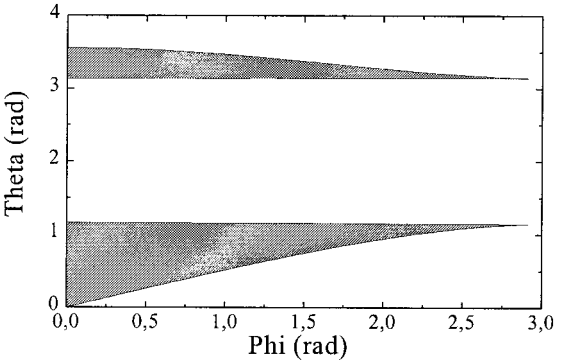

Figure 2 Dispersion diagram of an arbitrary unperturbed NLTL depicted in a reduced Brillouin zone

$$\cos \beta l = \cos kl - \frac{\omega C_{ls} Z_o}{2} \sin kl \tag{3}$$

where k (proportional to frequency) is the phase constant of the unloaded line. A representation of the dispersion relation for a typical NLTL is seen in Figure 2 in a Brillouin diagram, where the vertical axis corresponds to the electrical length of the unloaded line $\theta = kl$ (proportional to frequency), and the horizontal axis is the electrical length of the actual loaded line ($\varphi = \beta l$). From f_o and the dispersion relation, β can be determined and by applying the Bragg condition, so that λ_T is finally obtained. Provided we are interested on the analysis of the effects of an EBG on nonlinear propagation, rather than on the rejection of a specific frequency, we have set $\varphi = \beta l = \pi/2$. This gives a period for the perturbation which is a multiple of the distance between adjacent diodes $\lambda_T = 2l$ and eases the design of the EBG NLTL structure. According to Figure 2, a perturbation with such a period is expected to produce a frequency gap in the first passband near the cutoff frequency. The rejection level depends on the number of periods and the magnitude of the perturbation. Step variations of 40Ω up and down the nominal value of wave impedance ($Z_o = 104\Omega$) are expected to provide significant rejection in the EBG-related frequency gap. This wave impedance modulation is achieved by alternating the slot width between $G = 8.3$ mm (high impedance sections) and $G = 1.3$ mm (low impedance sections). With this, the geometry of the EBG NLTL is perfectly specified. Figure 3 shows the fabricated prototypes (NLTL and EBG NLTL), containing 10 diode-pair stages in order to generate significant harmonic content under large signal conditions. At the extremes of the devices, short (10 mm) 50Ω CPW sections have been cascaded to ensure a good matching at the ports.

3. RESULTS AND DISCUSSION

Actually, prior to the fabrication of the prototypes, linear and nonlinear simulations have been carried out by means of the commercial software ADS Agilent Technologies. As previously mentioned, slot-width modulation has been determined to produce step variations in wave impedance of $\Delta Z_o = 40\Omega$. This choice is explained from the simulated linear responses of several EBG NLTL structures with different perturbation levels (characterized by the variation of wave impedance). The varactors, which are included in the library of ADS Agilent Technologies, have been biased in all cases at 5 V to be

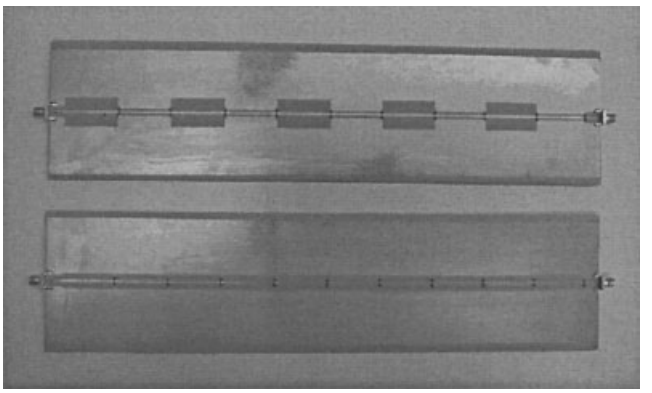

Figure 3 (a) Fabricated EBG NLTL and (b) unperturbed NLTL. The structures contain 10 diode stages to ensure significant harmonic content at the output under large signal conditions

consistent with the value of C_{ls}. The results, depicted in Figure 4, indicate that a band gap is opened near cutoff according to our expectations, centered at a frequency that slightly increases between 0.55 GHz ($\Delta Z_o = 10\Omega$) and 0.60 GHz ($\Delta Z_o = 50\Omega$). This shift is explained because the EBG structure itself introduces some dispersion, and this contribution becomes more important as the magnitude of the perturbation increases. This may also explain the slight variation of the Bragg frequency, which is obtained from the simulated frequency response. These simulations therefore indicate that under linear conditions, the EBG structure is able to significantly inhibit signal propagation in a certain gap. The center frequency of this forbidden band is related not only to the period of the perturbation, but also to line dispersion.

Let us now investigate the behaviour of the structure under large signal driving conditions where, due to nonlinearity, harmonics of the fundamental signal are produced. Our main aim is to analyze the ability of the structure to reduce the power transferred to those harmonics lying in the forbidden gap and how this affects other harmonics and the fundamental signal. To this end, harmonic balance simulations have been performed by means of ADS Agilent Technologies software, where the dc bias point of the diodes and the power of the driving signal have been set to 5 V and 22 dBm, respectively (simulations with lower power levels have also been carried out, but power interchange between harmonics is less significant). The results are shown in Figure 5, where the power of the fundamental, second, and third harmonic are depicted. These

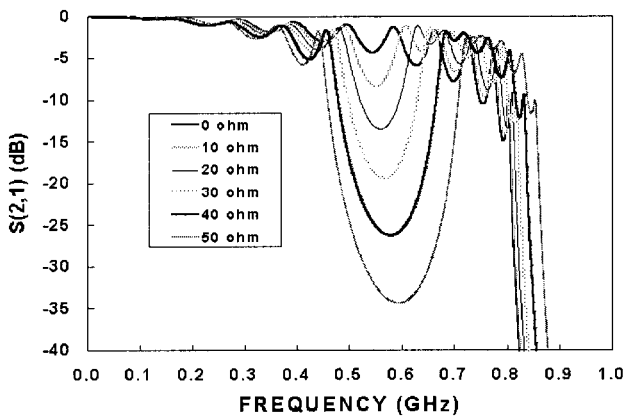

Figure 4 Simulated insertion loss for several EBG NLTLs with different levels of wave-impedance modulation. A frequency gap is clearly opened in the vicinity of 0.6 GHz

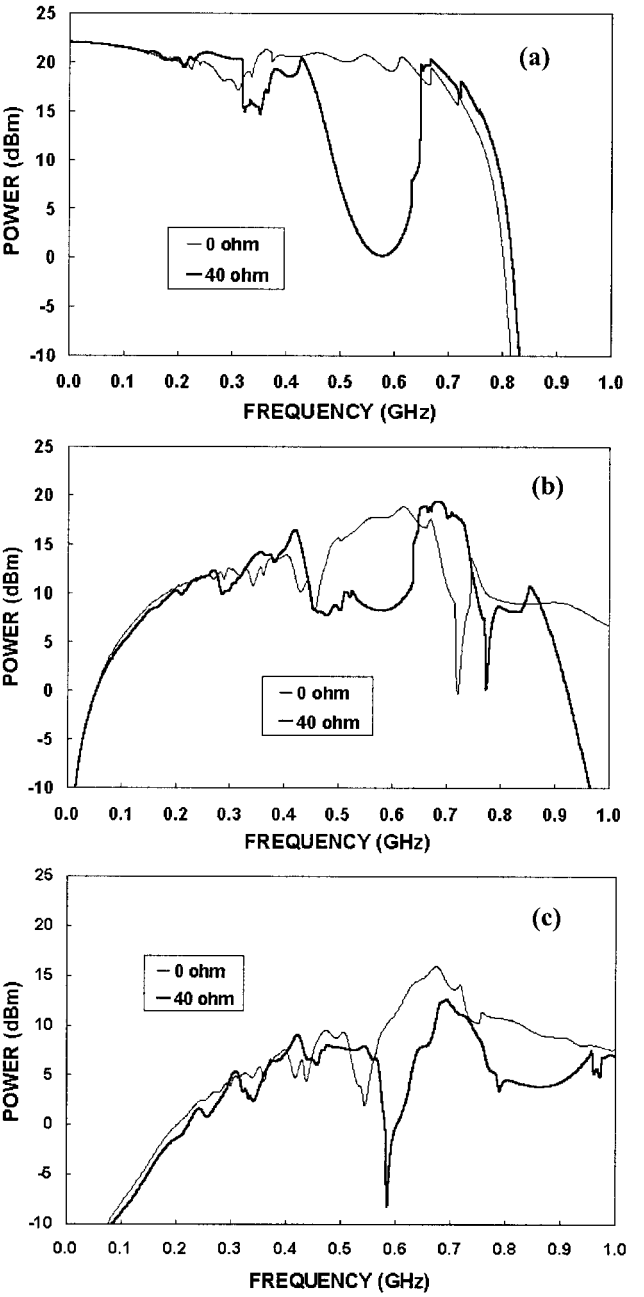

Figure 5 Harmonic balance simulations for the fabricated NLTL and EBG NLTL structures. The power level of the feeding signal is 22 dBm and signal frequency is swept up to 1 GHz. Output power is obtained for the (a) fundamental, (b) second, and (c) third harmonic. In (b) and (c) the horizontal axis is the frequency of the corresponding harmonic

results show that the power of the fundamental or that transferred to the second or third harmonic is decreased when the corresponding frequencies lie in the region where the EBG structure inhibits signal propagation—in the vicinity of 0.6 GHz. Therefore, according to these simulations, the reflection properties inherent to impedance modulation are also manifested under large signal driving conditions. A detailed analysis of Figure 5 points out an additional relevant feature that deserves special attention: when power conversion to the third harmonic is decreased as a consequence of the EBG action, power injected to the second harmonic is enhanced. This is clearly visible in Figure 5(b); which shows a frequency interval in the vicinity of 0.4 GHz that corresponds to third

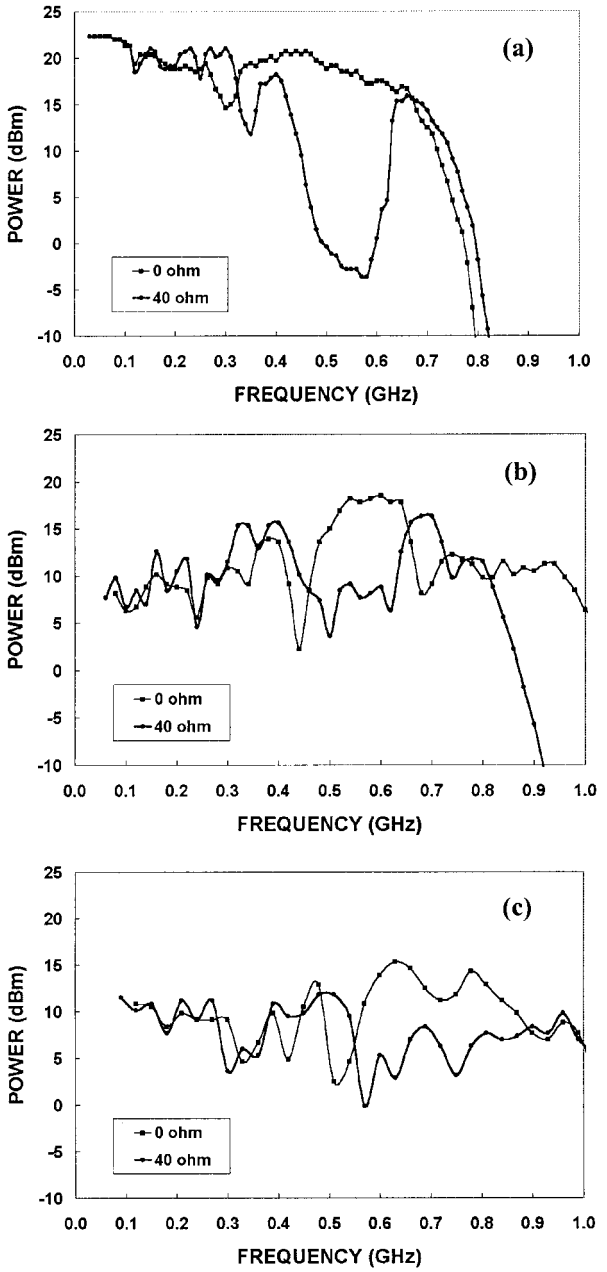

Figure 6 Nonlinear measurements for the fabricated NLTL and EBG NLTL structures. The power level of the feeding signal is 22 dBm and signal frequency is swept up to 1 GHz in step increments of 0.01 GHz. At each signal frequency, the power associated with the fundamental, second, and third harmonic is recorded. Output power is obtained for the (a) fundamental, (b) second, and (c) third harmonic. In (b) and (c) the horizontal axis is the frequency of the corresponding harmonic

harmonics lying near 0.6 GHz, that is, in the frequency gap introduced by the EBG structure. In other words, partial rejection of the third harmonic due to periodicity magnifies power conversion to the second harmonic. Inspection of Figure 5(a) reveals a similar behaviour, but in this case it is the degradation of the second harmonic which enhances the fundamental power in the vicinity of 0.3 GHz. This power enhancement of frequency products at the expense of higher-order harmonics has been obtained by the authors from harmonic balance simulations of other EBG NLTL structures with different electrical characteristics and nonlinear reactances and seems to be a general behaviour of EBG NLTLs. However, significant improvement of power conversion by means of an EBG structure at the expense of lower-order harmonics has not been found up to the present time. This different behaviour of power transfer in downward and upward frequency directions is under investigation, but it is thought to be due to the distributed nonlinearity of the EBG NLTL structure.

The effects of the EBG on frequency conversion have been experimentally obtained from the application of a 22-dBm feeding signal to the fabricated prototypes. An E4438C Agilent Technologies microwave source and Tektronix 2711 spectrum analyzer have been connected to the input and output ports of the devices. The results of the measurements, shown in Figure 6, confirm the degradation of those harmonics lying in the band gap of the EBG structure as well as the enhancement of the corresponding lower-order frequency products, in agreement with the harmonic balance simulations of Figure 5. To our knowledge, this is the first time that experimental results regarding the nonlinear behaviour of EBG NLTL structures has been presented. The results of this work indicate that the EBG action is effective under large signal regime, and conversion efficiency to a desired harmonic can be improved by designing the EBG structure to preclude the generation of higher-order frequency products.

4. CONCLUSION

In conclusion, the reflection properties of NLTLs periodically loaded with shunt-connected varactor diodes and perturbed by varying the slot width, have been investigated. These EBG NLTL structures have been found to inhibit signal propagation at the design frequencies even under large signal driving conditions (nonlinear regime). Harmonic balance simulations, as well as experimental results obtained from the application of large feeding signals to fabricated prototypes, have indicated that power transfer to those harmonics lying within the forbidden gap is degraded while conversion efficiency to lower frequency products is enhanced. These new type of structures, based on a double periodicity, can be of interest to add flexibility to the design of NLTL-based devices such as harmonic generators and time-delay phase shifters.

ACKNOWLEDGMENTS

This work has been supported by DGI and CICYT under project contracts BFM2001-2001 and TIC2002-04528-C02-01. Thanks to the DURSI (Generalitat de Catalunya) for supporting this work by means of an ACI Action ACI2001-33. Thanks to David Gonzalo (Agilent Technologies) for lending us the microwave source.

REFERENCES

1. H. Shi, W.M. Zhang, C.W. Domier, N.C. Luhmann, Jr., L.B. Sjogren, and H.X.L. Liu, Novel concepts for improved nonlinear transmission line performance, IEEE Trans Microwave Theory Techn 43 (1995), 780–788.
2. H. Yoneda, K. Tokuyama, K. Ueda, H. Yamamoto, and K. Baba, High power terahertz radiation with diamond photoconductive antenna array, 25th Int Conf Infrared Millimeter Waves Conf Dig, Beijing, 2002, p. 61.
3. M.J.W. Rodwell, M. Kamegawa, R. Yu, M. Case, E. Carman, and K.S. Giboney, GaAs nonlinear transmission lines for picosecond pulse generation and millimeter-wave sampling, IEEE Trans Microwave Theory Techn 39 (1991), 1194–1204.
4. J.R. Thorpe, P. Steenson, and R.E. Miles, Non-linear transmission lines for millimeter-wave frequency multiplier applications, IEEE Sixth Int Conf Terahertz Electron Proc 1998, pp. 54–57.
5. E. Lheurette, M. Fernández, X. Mélique, P. Mounaix, O. Vanbésien, and D. Lippens, Nonlinear transmission line quintupler loaded by heterostructure barrier varactors, Proc 29th Euro Microwave Conf Munich, 1999, pp. 217–220.

6. F. Martin, and X. Oriols, Simple model to study soliton wave propagation in periodic-loaded nonlinear transmission lines, Appl Phys Lett 78 (2001), 2802–2804.
7. M.J. Rodwell, S.T. Allen, R. Yu, M.G. Case, U. Bhattacharya, M. Reddy, E. Carman, M. Kamegawa, Y. Konishi, J. Pusl, and R. Pullela, Active and nonlinear wave propagation devices in ultrafast electronics and optoelectronics, Proc IEEE 82 (1994), 1037–1059.
8. M. Fernández, Nonlinear transmission lines for frequency multipliers applications, PhD. dissertation, Lille, France, 2001.
9. F. Martín, X. Oriols, J.A. Gil, and J. García.García, Optimization of nonlinear transmission lines for harmonic generation: the role of the capacitance-voltage characteristic and the area effect, Int J Infrared and Millimeter Waves 23 (2002), 95–103.
10. F.R. Yang, K.P. Ma, Y. Qian, and T. Itoh, A uniplanar compact photonic bandgap structure and its applications for microwave circuits, IEEE Trans Microwave Theory Tech 47 (1999), 1509–1514.
11. E. Peral, J. Capmany, and J. Martí, Iterative solution to the Gel' Fand-Levitan-Marchenko coupled equations and application to synthesis of fiber gratings, IEEE Journal of Quantum Electronics, 32 (1996), 2078–2084.
12. B.Z. Katsenelenbaum, L. Mercader, M. Pereyaslavets, M. Sorolla, and M. Thumm, Theory of nonuniform waveguides, ser. IEE Electromagn Waves London, U.K. IEE Press, 1998, vol. 44.
13. T. Lopetegi, M.A.G. Laso, J. Hernández, M. Bacaicoa, D. Benito, M.J. Garde, M. Sorolla, and M. Guglielmi, New microstrip wiggly-line filters with spurious passband suppression, IEEE Transaction on Microwave Theory Tech 49 (2001), 1593–1598.
14. V. Radisic, Y. Qian, and T. Itoh, Broad-band power amplifier using dielectric photonic bandgap structures, IEEE Microwave Guided Wave Lett 8 (1998), 13–15.
15. Y.-T. Lee, J.-S. Lim, J.-S. Park, D. Ahn, and S. Nam, A novel phase noise reduction technique in oscillators using defected ground structure, IEEE Microwave Wireless Comp Lett 12 (2002), 39–41.
16. Y.-Q. Fu, G.H. Zhang, and N.C. Yuan, A novel PBG coplanar waveguide, IEEE Microwave and Wireless Components Lett 11 (2001), 447–449.
17. T.-Y. Yun and K. Chang, Uniplanar one-dimensional photonic bandgap structures and resonators, IEEE Trans Microwave Theory Tech 49 (2001), 549–553.
18. A. Görür, C. Karpuz, and M. Alkan, Characteristics of periodically loaded CPW structures, IEEE Microwave Guided Wave Lett 8 (1998), 278–280.
19. S.G. Mao and M.Y. Chen, A novel periodic electromagnetic bandgap structure for finite-width conductor backed coplanar waveguides, IEEE Microwave and Wireless Components Lett 11 (2001), 261–263.
20. J. Sor, Y. Qian, and T. Itoh, Miniature low-loss CPW periodic structures for filter applications, IEEE Trans Microwave Theory Tech 49 (2001), 2336–2341.
21. F. Martín, F. Falcone, J. Bonache, T. Lopetegi, M.A.G. Laso, and M. Sorolla, New periodic-loaded electromagnetic bandgap coplanar waveguide with complete spurious passband suppression, IEEE Microwave and Wireless Components Lett 12 (2002).
22. F. Martín, F. Falcone, J. Bonache, T. Lopetegi, M.A.G. Laso, M. Coderch, and M. Sorolla, Periodic-loaded sinusoidal patterned electromagnetic bandgap coplanar waveguides, Microwave and Optical Technology Letters, to be published.
23. M. Fernández, F. Martín, P. Steenson, X. Melique, A. Oistein, X. Oriols, O. Vanbesien, J. García-García, R. Miles, and D. Lippens, A comparison of different approaches for the simulation of nonlinear transmission lines, Microwave and Optical Tech Lett 33 (2002), 134–136.
24. A. Oliner, Types and basic properties of leaky modes in microwave and millimeter wave integrated circuits, IEICE Trans Electron E83-C (2000), 675–686.
25. D.M. Pozar, Microwave engineering, Addison-Wesley, Reading, MA, 1990.

A WIDEBAND MEANDER-LINE PROBE-FED PATCH ANTENNA

B. L. Ooi and C. L. Lee
National University of Singapore
Department of Electrical and Computer Engineering
10 Kent Ridge Crescent
Singapore 119260

Received 3 December 2002

ABSTRACT: *In this paper, the characteristics of a bent meander-line probe fed patch antenna are investigated. The air-filled patches are designed at a height of about 9% of the wavelength and the bent meander-line probe fed antenna is able to achieve an impedance bandwidth of about 31% for a VSWR of less than 2. The four basswoods, which support the microstrip patch, are noticed experimentally to have little effect on the overall performance. The in-band return loss of the proposed antenna is found experimentally to be better than the recently proposed L-shaped probe patch antenna.* © 2003 Wiley Periodicals, Inc.
Microwave Opt Technol Lett 37: 401–403, 2003; Published online in Wiley InterScience (www.interscience.wiley.com). DOI 10.1002/mop.10930

Key words: *meander-line; patch antenna; broad band antenna*

1. INTRODUCTION

The major drawback of a rectangular patch antenna in its basic form is its inherently narrow bandwidth. Several techniques have been proposed in the literature for widening the bandwidth. These include the addition of parasitic patches, the usage of thick substrate, and the addition of multi-layer patches. Quite recently, an L-shaped probe patch antenna [1] with an impedance bandwidth of 35% was proposed. A novel broadband air-filled U-slot patch antenna using the L-shaped probe [2] to improve the bandwidth and gain has also been proposed recently. These two methods have also been combined with stacking of rectangular patches [3] to increase the overall impedance bandwidth to about 44%. In this paper, an alternate design that uses a bent meander-line probe is proposed. It will be demonstrated experimentally that with the used of this feed, an improvement to the overall in-band return loss of lower than −15 dB is achieved. A comparison of the L-shaped probe patch antenna with the novel bent meander-line probe-fed patch antenna is also made in this paper.

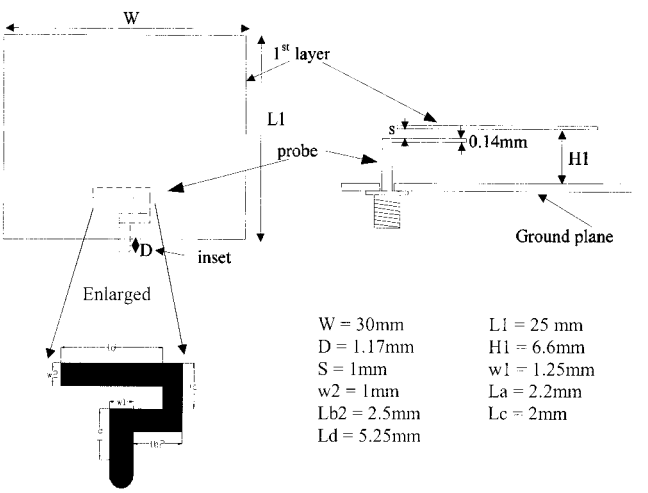

Figure 1 Antenna geometry of the bent meander-line probe-fed patch antenna